Budapest University of Technology and Economics
Department on Manufacturing Sciences and Technology

Booklet of PhD Theses

An analysis of the machinability of die-cast aluminium alloys in the fine turning of external cylindrical surfaces

Horváth Richárd
2015.

Leader: Dr. Stépán Gábor, full professor, a regular member of the Hungarian Academy of Sciences

Supervisor: Dr. Mátyási Gyula, honorary professor

Contents

1 Introduction

Aluminium (and aluminium alloy) products are becoming more and more widely used. The car industry, the aviation industry and the military are steadily increasing their use of aluminium alloys due to their numerous excellent mechanical and chemical properties. The final machining of aluminium products (or one of their selected areas) is often done with turning. As a result, I carried out my investigations on two types of die cast aluminium alloys (silumins).

2 Research Goals

Among my goals are the examination of the machinability of the materials used and the cutting ability of the tools. In more detail:

- The examination of the widely used surface roughness parameters *Ra* and *Rz* and the creation of a phenomenological model to estimate these, which contains insert edge material and machined materials as qualitative variables in addition to the usual cutting parameters.
- It is not enough to minimize surface roughness during manufacturing, it is advisable to reduce its deviation, too (robust planning). Therefore I extended my research to the deviation of measured surface roughness parameters.
- The statistical measures of surface roughness (*Rsk*, *Rku*) greatly influence the tribological characteristics of working surfaces, so I included the analysis of the statistical measures of surface roughness in my investigations.
- The literature distinctly separates on the topological map surfaces manufactured with different technologies (Fig. 1.). I set out to investigate the topological map of fine turning with tools of different edge material and edge geometry.

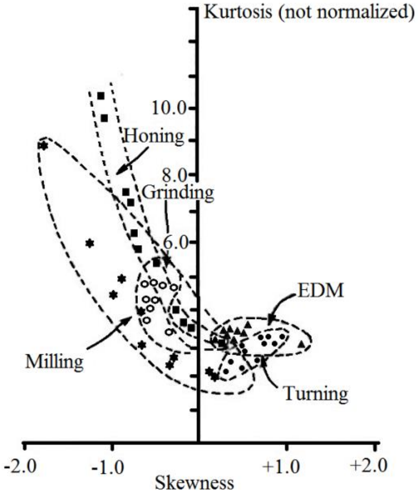

Fig. 1. A topological map of surfaces made with various cutting methods

- Another goal of my investigations was the analysis of the deviation of the statistical parameters of surface roughness.
- In fine turning the cutting length of the edge of the tool is less than the nose radius or is comparable to it, therefore I investigated how chip cross-section can be better defined at depths of cut comparable to the nose radius of the tool.
- The building of a force model for the conditions of fine turning (in the case of the materials examined: AS12; AS17) which operates with dimensions characteristic of chip cross-sections in fine turning.
- The designing, building checking and adapting of a special three-component dynamometer system covering the range of aluminium fine turning.

3 Materials and methods

3.1 Materials used in the experiments

Two die-cast aluminium alloys were used in the experiments:

The chemical composition of the AS12 eutectic alloy (in wt %) is: Al = 88.54 %; Si = 11.46 %. Its hardness is: $67 \pm 2HB_{2.5/62.5/30}$.

The chemical composition of the AS17 hypereutectic alloy (in wt %) is: Al = 79.44 %; Si = 18.21 %, Cu = 1,09 %; Mg = 0.45%. Its hardness is: 114±3 $HB_{2.5/62.5/30}$.

3.2 Tools used in the experiments

Diamond tools were used in the experiments (insert code: DCGW 11T304). I used tools of three edge materials: polycrystalline diamond (PCD), chemical vapour deposition diamond (CVD-D), and synthetic monocrystalline diamond (MDC). I examined these tools with both conventional (ISO) and non-conventional (Wiper) geometry (Fig. 2.).

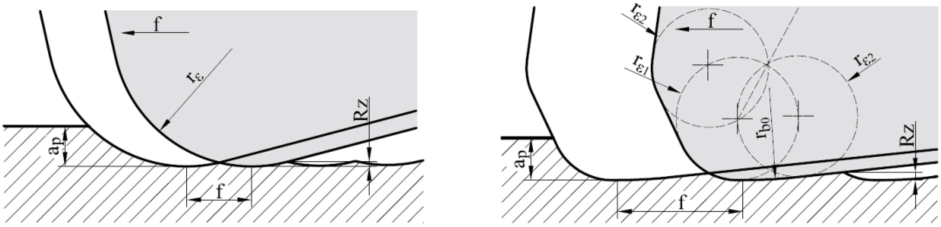

a) b)

Fig. 2. Theoretical geometries of ISO and Wiper edges; a) conventional (ISO) geometry; b) non-conventional (Wiper) geometry; *f* - feed, a_p - depth of cut, r_ε radius of the cutting edge, $r_{\varepsilon 1}$ and $r_{\varepsilon 2}$ radii of wiper curvature, r_{b0} radius of smoothing part, *Rz* surface height

Table 1. summarizes the tools used.

Table 1. Tools used in the experiments (x)

		edge material		
		PCD	CVD-D	MDC
edge geometry	ISO	x	x	x
	Wiper	x	x	-

3.3 Machine tools used in the experiments

Surface roughness experiments were carried out on a EuroTurn 12B CNC lathe, while cutting force measurements were performed on a Dugard Eagle BNC 1640 CNC lathe.

3.4 The roughness tester used

The roughness of the turned surfaces was measured with a Mitutoyo SJ301 surface roughness tester. Surface roughness was measured 12 times along the circumference of the workpieces (at 30 degrees) and the surface roughness values are the averages of the values at these 12 measurement points.

3.5 The design of experiments used

When using the Response Surface Method (RSM), I used a Central Composite Design (CCD). The basis of the DOE is a design of 16 experiments, in which three cutting parameters (cutting speed v_c, m/min; feed f, mm; depth of cut a_p, mm) were varied systematically, including measurement at a central point and its repeated measurement (Fig. 3, Table 2).

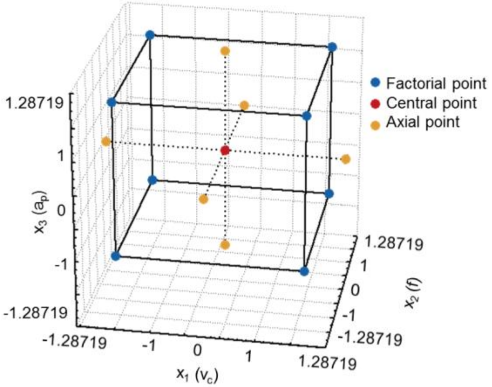

Fig. 3. Experiment points [S1]

Table 2. The levels of the experiment points

Experiment points N	v_c	f	a_p
1	-1	-1	-1
2	-1	-1	1
3	-1	1	-1
4	-1	1	1
5	1	-1	-1
6	1	-1	1
7	1	1	-1
8	1	1	1
9	1.28719	0	0
10	1.28719	0	0
11	0	-1.28719	0
12	0	1.28719	0
13	0	0	-1.28719
14	0	0	1.28719
15 (C)	0	0	0
16 (C)	0	0	0

Double feed was used with Wiper geometry tools so that surface roughness values were comparable. The values of cutting parameters can be found in Table 3.

Table 3. The levels of cutting parameters

	-1.28719	-1	0	1	1.28719
v_c, m/min	500	667	1250	1833	2000
f_{ISO}, mm	0.05	0.058	0.085	0.112	0.12
f_{Wiper}, mm	0.1	0.116	0.17	0.224	0.24
a_p, mm	0.2	0.267	0.5	0.733	0.8

Tables 2. and 3. yield the 16 experiments for ISO and Wiper tools (which only differ in feed) (Tables 4. and 5.).

Table 4. DOE for ISO edge geometry tools

Experimental runs, N	**v_c, m/min**	**f, mm**	**a_p, mm**
1	667	0.058	0.267
2	667	0.058	0.733
3	667	0.112	0.267
4	667	0.112	0.733
5	1833	0.058	0.267
6	1833	0.058	0.733
7	1833	0.112	0.267
8	1833	0.112	0.733
9	500	0.085	0.5
10	2000	0.085	0.5
11	1250	0.05	0.5
12	1250	0.12	0.5
13	1250	0.085	0.2
14	1250	0.085	0.8
15	1250	0.085	0.5
16	1250	0.085	0.5

Table 5. DOE for Wiper edge geometry tools

Experimental runs, N	**v_c, m/min**	**f, mm**	**a_p, mm**
1	667	0.116	0.267
2	667	0.116	0.733
3	667	0.224	0.267
4	667	0.224	0.733
5	1833	0.116	0.267
6	1833	0.116	0.733
7	1833	0.224	0.267
8	1833	0.224	0.733
9	500	0.17	0.5
10	2000	0.17	0.5
11	1250	0.1	0.5
12	1250	0.24	0.5
13	1250	0.17	0.2
14	1250	0.17	0.8
15	1250	0.17	0.5
16	1250	0.17	0.5

3.7 The building of united models

In order to facilitate technological planning, it is advisable to build united models which include the workpiece materials, as well as tool edge materials as input parameters. The following united model was developed for the results:

$$Y = \Omega(v_c, f, a_p, TM, WM) \qquad (1)$$

where TM is the tool material and WM is the workpiece material. The values of these quality parameters can be found in Table 6.

Table 6. The variables of the workpiece materials used

	AS12	AS17	
WM – workpiece material	0	1	
	PCD	CVD	MDC
TM – tool material	0	1	2

The united phenomenological models are as follows:

$$\begin{aligned} Ra &= d_0 + d_1 \cdot WM + d_2 \cdot TM + d_3 \cdot v_c + d_4 \cdot f + d_5 \cdot a_p + d_{22} \cdot TM^2 + d_{33} \cdot v_c^2 + d_{44} \cdot f^2 + \\ &+ d_{55} \cdot a_p^2 + d_{12} \cdot WM \cdot TM + d_{13} \cdot WM \cdot v_c + d_{14} \cdot WM \cdot f + d_{15} \cdot WM \cdot a_p + d_{23} \cdot TM \cdot v_c + \\ &+ d_{24} \cdot TM \cdot f + d_{25} \cdot TM \cdot a_p + d_{34} \cdot v_c \cdot f + d_{35} \cdot v_c \cdot a_p + d_{45} \cdot f \cdot a_p + \varepsilon \end{aligned} \tag{2}$$

$$\begin{aligned} Rz &= e_0 + e_1 \cdot WM + e_2 \cdot TM + e_3 \cdot v_c + e_4 \cdot f + e_5 \cdot a_p + e_{22} \cdot TM^2 + e_{33} \cdot v_c^2 + e_{44} \cdot f^2 + \\ &+ e_{55} \cdot a_p^2 + e_{12} \cdot WM \cdot TM + e_{13} \cdot WM \cdot v_c + e_{14} \cdot WM \cdot f + e_{15} \cdot WM \cdot a_p + e_{23} \cdot TM \cdot v_c + \\ &+ e_{24} \cdot TM \cdot f + e_{25} \cdot TM \cdot a_p + e_{34} \cdot v_c \cdot f + e_{35} \cdot v_c \cdot a_p + e_{45} \cdot f \cdot a_p + \varepsilon \end{aligned} \tag{3}$$

where d_0; d_i; d_{ij}; e_0; e_i; e_{ij} are the calculated coefficients and ε is the experimental error.

3.8 The calculation of optimum with desirability functions

Productivity can be defined as cutting speed multiplied by feed. The combined optimum of the following three target functions:

$$Ra \Rightarrow Min \tag{4}$$

$$Rz \Rightarrow Min \tag{5}$$

$$Pf = v_c \cdot f \Rightarrow Max \tag{6}$$

can be calculated with desirability functions. Desirability functions can take a value between 0 and 1. The higher the desirability value, the closer we are to the expected value. The desirability functions selected in my investigations are d_{Ra}, d_{Rz} and d_{Pf} (Fig. 4.).

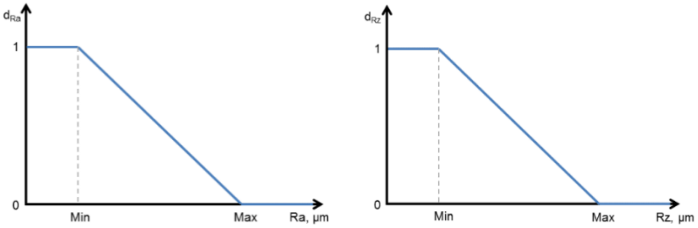

a) Desirability of *Ra*

b) Desirability of *Rz*

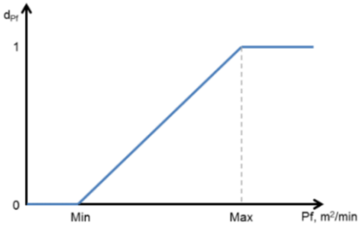

c) Desirability of *Pf*

Fig. 4. Desirability functions

With the composite desirability function (*D*) the optimum of the criteria can be found as follows:

$$D = \sqrt[3]{d_{Ra} \cdot d_{Rz} \cdot d_{Pf}} \tag{7}$$

where the value of *D* is maximal, there is the combined optimum of the three target functions.

4 A dynamic model for fine turning

I introduced two parameters for chip cross-sections characteristic to fine turning (h_{eq} – equivalent chip thickness; l_{eff} – effective edge length) (Fig. 5.).

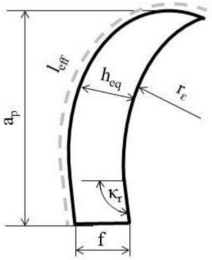

Fig. 5. Characteristic chip cross-section in the case of fine turning [S5]

In the case of fine turning effective edge length can be calculated with the following formula:

$$l_{eff} = \frac{a_p - r_\varepsilon \cdot (1 - \cos\kappa_r)}{\sin\kappa_r} + \frac{2 \cdot r_\varepsilon \cdot \pi}{360°} \cdot \left(\kappa_r + \arcsin\frac{f}{2 \cdot r_\varepsilon} \right) \tag{8}$$

Equivalent chip thickness is therefore the following:

$$h_{eq} = \frac{a_p \cdot f}{l_{eff}} \tag{9}$$

In fine turning h_{eq}<<1 mm is always true, therefore $k_{1.1}$ cannot be used. For this reason, I introduced the parameter main specific cutting force $k_{1,0.1}$, which applies to $l_{eff} = 1\ mm$ and $h_{eq} = 0{,}1\ mm$.

The cutting force model introduced requires the calculation of specific cutting force using the force measured with the dynamometer:

$$k = \frac{F}{A} = \frac{F}{h_{eq} \cdot l_{eff}} \tag{10}$$

The obtained values of k, however, depend on the values of h_{eq} and l_{eff}, therefore they were modelled with two-factor power function regression:

$$k = C \cdot h_{eq}{}^{q} \cdot l_{eff}{}^{y} \tag{11}$$

If $h_{eq}=0{,}1\ mm$ is applied, the value of $k_{1,0.1}$ is the following:

$$k_{1,0.1} = C \cdot 0{,}1^{q} \tag{12}$$

And from this, the cutting force model sought [S5]:

$$F = k \cdot h_{eq} \cdot l_{eff} = k_{1,0.1} \cdot 10^{q} \cdot h_{eq}{}^{1+q} \cdot l_{eff}{}^{1+y} \tag{13}$$

The 21st point in the series of experiments (Table 7.) is to determine (check) the value of $k_{1,0.1}$.

Table 7. Experiment points of the dynamic examinations

Measurement point	***a_p, mm***	***f, mm***	***l_{eff}, mm***	***h_{eq}, mm***	***A, mm^2***
1.	0,25	0,03	0,493	0,015	0,0075
2.	0,25	0,05	0,503	0,025	0,0125
3.	0,25	0,07	0,513	0,034	0,0175
4.	0,25	0,09	0,523	0,043	0,0225
5.	0,25	0,11	0,533	0,052	0,0275
6.	0,25	0,13	0,543	0,060	0,0325
7.	0,25	0,15	0,554	0,068	0,0375
8.	0,5	0,03	0,743	0,020	0,015
9.	0,5	0,05	0,753	0,033	0,025
10.	0,5	0,07	0,763	0,046	0,035
11.	0,5	0,09	0,774	0,058	0,045
12.	0,5	0,11	0,784	0,070	0,055

Measurement point	*a_p, mm*	*f, mm*	*l_{eff}, mm*	*h_{eq}, mm*	*A, mm^2*
13.	0,5	0,13	0,794	0,082	0,065
14.	0,5	0,15	0,804	0,093	0,075
15.	0,7	0,03	0,944	0,022	0,021
16.	0,7	0,05	0,954	0,037	0,035
17.	0,7	0,07	0,964	0,051	0,049
18.	0,7	0,09	0,974	0,065	0,063
19.	0,7	0,11	0,984	0,078	0,077
20.	0,7	0,13	0,994	0,092	0,091
($k_{1,0.1}$) 21.	0,7	0,143	1,001	0,100	0,1001
22.	0,7	0,15	1,004	0,105	0,105

5 Designing and adapting a dynamometer to measure cutting forces in fine turning

5.1 Requirements the dynamometer has to meet

Measurements of force were carried out with a dynamometer designed and adapted to the technology of fine turning. Fig. 5 shows the exploded view of the dynamometer.

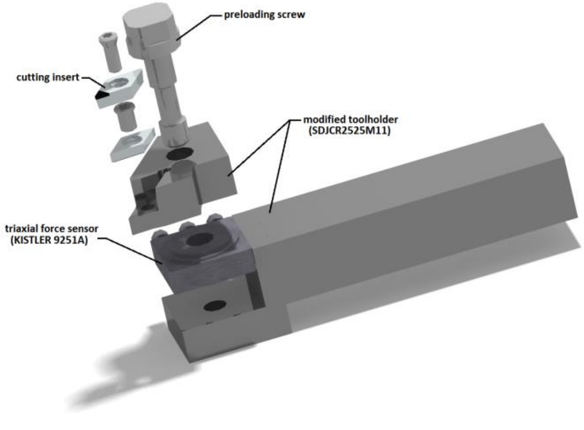

Fig. 5. An exploded view of the modified toolholder

The sensitivities (pC/N) belonging to the force components were determined.

In the planned range of the dynamometer (0…100N) I took the error curve for all three force components (Fig. 6).

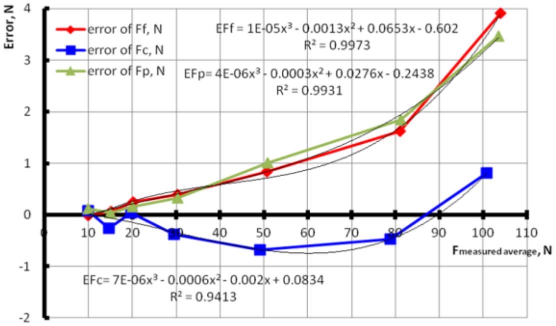

Fig. 6. The error curves of force components F_c, F_f and F_p in the planned range [S10]

The error curve can be used to modify and correct measurement results.

6 Results

6.1 *Ra* and *Rz* roughness parameter results

The combined and reduced equations are the following [S1]:

$$\begin{aligned} Ra_{ISO} &= 5.76\cdot10^{-1} + 2.510\cdot10^{-1}\cdot WM + 3.687\cdot10^{-2}\cdot TM + 3.694\cdot10^{-4}\cdot v_c - 14.81\cdot f \\ &+ 3.753\cdot10^{-2}\cdot a_p - 1.019\cdot10^{-1} TM^2 - 1.430\cdot10^{-7}\cdot v_c^2 + 184.3\cdot f^2 + 4.679\cdot10^{-2}\cdot WM\cdot TM \\ &- 5.191\cdot10^{-5}\cdot WM\cdot v_c - 2.306\cdot WM\cdot f + 8.865\cdot10^{-5}\cdot TM\cdot v_c + 4.702\cdot10^{-1}\cdot TM\cdot f \\ &- 1.151\cdot10^{-3}\cdot v_c\cdot f \end{aligned} \tag{14}$$

(R^2=0.8621)

$$\begin{aligned} Rz_{ISO} &= 1.717\cdot10^{-1} + 1.421\cdot WM - 2.333\cdot10^{-1}\cdot TM + 2.475\cdot10^{-3}\cdot v_c - 11.36\cdot f \\ &+ 1.013\cdot a_p - 4.937\cdot10^{-1}\cdot TM^2 - 6.934\cdot10^{-7}\cdot v_c^2 + 532.2\cdot f^2 \\ &+ 1.354\cdot10^{-1}\cdot WM\cdot TM - 1.735\cdot10^{-4}\cdot WM\cdot v_c - 14.10\cdot WM\cdot f \\ &+ 2.903\cdot10^{-4}\cdot TM\cdot v_c + 8.249\cdot TM\cdot f + 2.437\cdot10^{-1}\cdot TM\cdot a_p - 1.1653\cdot10^{-2}\cdot v_c\cdot f - 12.69\cdot f\cdot a_p \end{aligned} \tag{15}$$

(R^2=0.8384)

$$\begin{aligned} Ra_{Wiper} &= 1.150 + 1.445\cdot10^{-1}\cdot WM + 1.569\cdot10^{-1}\cdot TM - 3.291\cdot10^{-4}\cdot v_c \\ &- 7.799\cdot f - 1.023\cdot a_p + 9.717\cdot10^{-8}\cdot v_c^2 + 31.06\cdot f^2 \\ &+ 7.602\cdot10^{-1}\cdot a_p^2 - 1.263\cdot WM\cdot f - 4.718\cdot10^{-5}\cdot TM\cdot v_c - 7.103\cdot10^{-1}\cdot TM\cdot f \\ &+ 8.152\cdot10^{-4}\cdot v_c\cdot f + 2.463\cdot f\cdot a_p \end{aligned} \tag{16}$$

(R^2=0.7857)

$$\begin{aligned} Rz_{Wiper} = {} & 3.041 - 2.991 \cdot 10^{-1} \cdot WM + 2.042 \cdot 10^{-2} \cdot TM - 9.093 \cdot 10^{-4} \cdot v_c \\ & - 2.103 \cdot f - 1.064 \cdot a_p + 3.131 \cdot 10^{-7} \cdot v_c^2 + 52.65 \cdot f^2 + 1.010 \cdot a_p^2 \\ & + 2.133 \cdot 10^{-4} \cdot WM \cdot v_c - 3.298 \cdot WM \cdot f + 5.701 \cdot 10^{-1} \cdot WM \cdot a_p - 2.951 \cdot TM \cdot f \end{aligned} \tag{17}$$

(R^2=0.7742)

Equations (14), (15), (16) and (17) describe the surface roughness parameters (*Ra*, *Rz*) well in the case of the ISO and Wiper geometry tools. If these equations are used, the surface roughness obtained by fine turning can be determined with the cutting parameters and the workpiece material and the edge material.

Fig. 7. illustrates how the combined reduced mathematical models (14), (15), (16) and (17) behave as cutting speed and feed are varied.

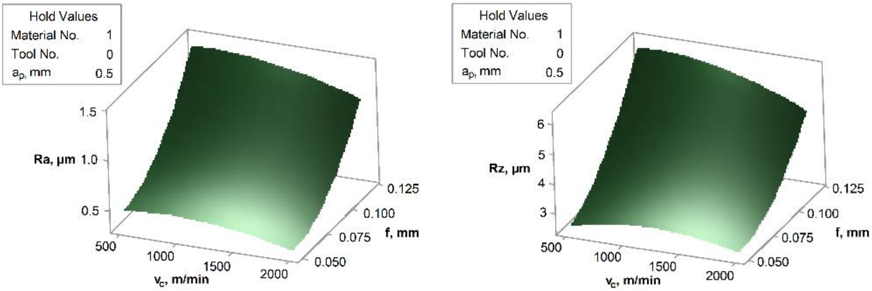

diagram of eq. (14), material: AS17; tool: PCD-ISO

diagram of eq. (15), material: AS17; tool: PCD-ISO

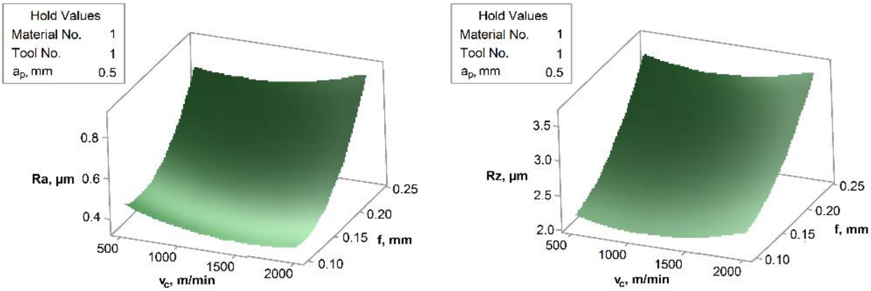

diagram of eq. (16), material: AS17; tool: CVD-D-Wiper

diagram of eq. (17), material: AS17; tool: CVD-D-Wiper

Fig. 7. A graphic representation of the combined reduced equations [S1]

6.2 Determining the optimum with desirability functions

The desirability functions for optimization are the following:

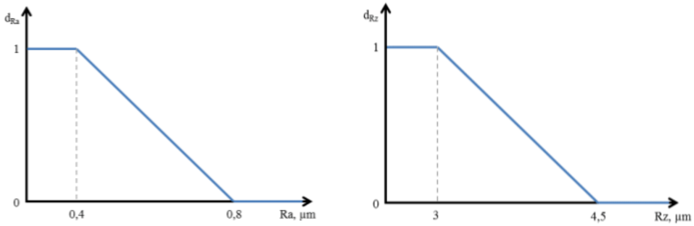

a) The desirability function of *Ra* b) The desirability function of *Rz*

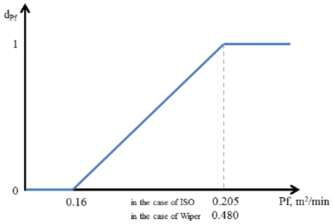

b) The desirability function of *Pf*

Fig. 8. Desirability functions [S1]

Having carried out optimization, we obtained the following values for ISO cutting tools:

WM = 1 (AS17), and TM = 0 (PCD). The cutting parameters to be set are: v_c = 2000 m/min, f = 0.089 mm, and a_p = 0.2 mm. The surface roughness parameters and productivity to be achieved are: *Ra* = 0.579 µm, *Rz* = 3.301 µm, and *Pf* = 178 m^2/min.

In the case of desirability functions *dRa* = 0.552; *dRz* = 0,799; *dPf* =0.426, and composite desirability D = 0.573.

In the case Wiper cutting tools the results are as follows:

WM = 1 (AS17), and TM = 1 (CVD). The cutting parameters to be set are: v_c = 2000 m/min, f = 0.158 mm, a_p = 0.42 mm. The surface roughness parameters and productivity to be achieved are: *Ra* = 0.444 µm, *Rz* = 2.587 µm, *Pf* = 315.9 m^2/min.

In the case of desirability functions *dRa* = 0.889; *dRz* = 1; *dPf* = 0.516, while composite desirability *D* = 0.771.

Once the optimal level of the design parameters has been determined, the final step of our investigations is to verify the obtained results. To achieve this, confirmation tests were carried out. The differences between the measured and the estimated *Ra* values are quite small. The measured *Rz* value in the case of the ISO cutting tool is lower, in the case of the Wiper cutting tool it is higher than the estimated values, but the magnitude of this difference is not notable in technological planning.

6.3 The analysis of the statistical parameters of surface roughness (*Rsk*, *Rku*)

The statistical parameters of surface roughness (*Rsk*, *Rku*) also come from the evaluation of the 12 measurements. Each point of the topological map (Fig. 9.) is the average of these 12 points, grouped by edge geometry.

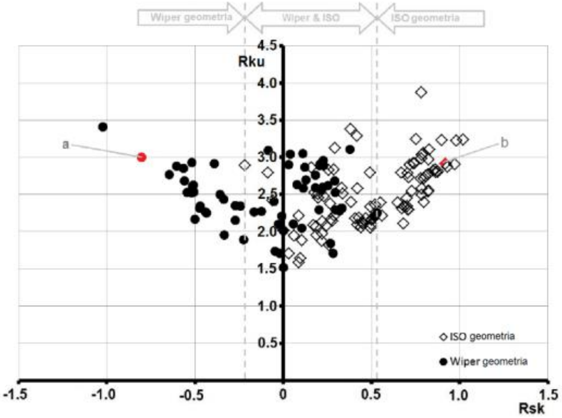

Fig. 9. Topological maps of surfaces manufactured with different edge geometry tools [S2]

Table 8. The range of *Rsk* values as a function of edge geometries [S2]

Wiper geometry	Wiper & ISO geometry	ISO geometry
-1…-0.2	-0.2…0.55	0.55…1.0

Three distinct *Rsk* ranges can be observed on the topological map (Fig. Fig. **9.** and Table Table **8.**).

Two surface profiles can be seen in Fig. 10. These profiles represent the surfaces found in the topological map of points a and b in Fig. 9. The cutting parameters of these profiles – as shown in Fig. 10 – are similar to each other. There are differences only in feed and tool geometry. The profile cut by a tool with ISO geometry is shown in Fig. 10.a. Tool marks show a typical turned character with high, sharp peaks. The surface produced by a Wiper tool has a plateau-like character (Fig. 10.b). The tool – as is well-known – flattens the surface. This flattening effect comes from the special tool geometry. It can be observed in Fig. 2. that because of the radius r_{b0} connecting the radii $r_{\varepsilon 1}$ and $r_{\varepsilon 2}$ of Wiper geometry, the edge part in depth has a smaller end cutting edge angle than in the case of ISO geometry. In this case surface height (*Rz*) is lower. As a result of this effect, the high peaks disappear and the surface becomes finer, that is why the productivity of Wiper tools is higher. But there is another effect: the flatting process forms a plateau-like surface, which means a better tribological behaviour as real contact in the frictional process is much higher in the case of a plateau-like surface than in case of a surface with high, sharp peaks.

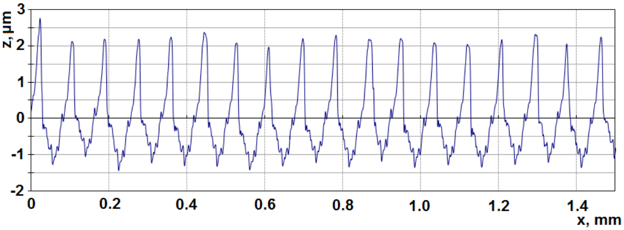

a) Turned profile produced with ISO geometry
(surface roughness parameters: *Ra* = 0,806 µm; *Rz* = 4,056 µm; *Rsk* = 0,917; *Rku* = 2,915
cutting parameters: v_c = 500 m/min; *f* = 0,085 mm; a_p = 0,5 mm)

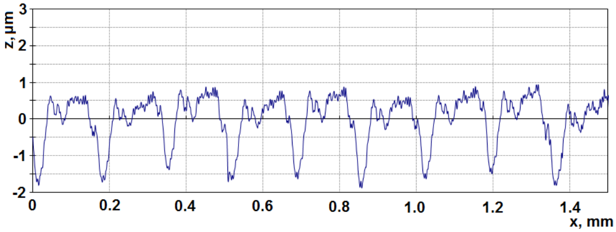

b) Turned profile produced with Wiper geometry
(surface roughness parameters: *Ra* = 0,493 µm; *Rz* = 2,783 µm; *Rsk* = -0,803; *Rku* = 2,995
cutting parameters: v_c = 500 m/min; *f* = 0,17 mm; a_p = 0,5 mm)

Fig. 10. Profiles with different Rsk-Rku values [S2]

6.4 The results of the dynamic experiments

Dynamic experiments were carried out as described in chapter 4. Dynamic investigations were carried out with the tool used in optimum search (edge material: PCD, edge geometry: ISO).

Based on the dynamic model (13) presented (in chapter 4.) the following equations were built to estimate the three force components (for the different materials) [S5]:

$$F_{c\_AS12} = 692 \cdot 10^{-0,198} \cdot h_{eq}^{\;0,8} \cdot l_{eff}^{\;0,96} \tag{18}$$

$$F_{c\_AS17} = 763 \cdot 10^{-0,272} \cdot h_{eq}^{\;0,728} \cdot l_{eff}^{\;1,089} \tag{19}$$

$$F_{f\_AS12} = 112 \cdot 10^{-0,607} \cdot h_{eq}^{\;0,393} \cdot l_{eff}^{\;0,153} \tag{20}$$

$$F_{f\_AS17} = 135 \cdot 10^{-0,657} \cdot h_{eq}^{\;0,343} \cdot l_{eff}^{\;0,221} \tag{21}$$

$$F_{p\_AS12} = 202 \cdot 10^{-0,66} \cdot h_{eq}^{\;0,34} \cdot l_{eff}^{\;1,43} \tag{22}$$

$$F_{p\_AS17} = 226 \cdot 10^{-0,752} \cdot h_{eq}^{\;0,248} \cdot l_{eff}^{\;1,44} \tag{23}$$

The model created for component F_c showed the greatest accuracy in the case of both materials but the models also describe force components F_f and F_p with adequate accuracy for technological planning.

The following can be said about the force model I introduced and adapted to fine turning:

- The force model operates with chip sizes characteristic to fine turning (I introduced the parameters h_{eq} – equivalent chip thickness and l_{eff} – effective edge length).
- With formula (11) of the specific cutting force that I introduced specific force values can be calculated very accurately in the case of all three components.
- Main specific cutting force values can be calculated easily with formula (12) for fine turning.
- The experiments show that the equations of cutting force components (based on 13) describe and model measured force values with great accuracy.

7 Theses

Thesis 1.

I created for fine turning 4 combined reduced phenomenological models to estimate surface roughness parameters *Ra* and *Rz* within the range of cutting parameters in the experiments. The phenomenological models also include workpiece materials and edge materials of the tools used, as qualitative, discreet variables, in addition to cutting parameters. With these phenomenological models the expected value of *Ra* and *Rz* surface roughness parameters can be estimated in preliminary technological planning. The investigated workpiece materials: AS12 and AS17 aluminium alloys. The edge materials of the cutting tools used: PCD, CVD-D, and MCD. The cutting parameter range: v_c=500-2000 m/min; f_{ISO}=0.05-0.12 mm; f_{Wiper}=0.1-0.24 mm; a_p=0.2-0.8 mm.

Thesis I. is based on the following publications: [S1][S3][S4][S7][S11][S12][S16][S17]

Thesis 2.

I defined desirability functions for the surface roughness to be achieved in fine turning (*Ra* and *Rz*), and productivity, using which I defined an optimum for the two edge geometries. Optimization covered cutting speed, depth of cut, feed, edge material, and workpiece material. The investigated parameter range and the conditions are identical to those in thesis 1.

Thesis II. is based on the following publications: [S1][S3][S4][S13][S17]

Thesis 3.

I proved with experiments that the statistical parameters of surface roughness (*Rsk*, *Rku*), which have a great influence on the characteristics of working surfaces, only depend on edge geometry in the investigated technological range. The topological map of fine turning I examined can be divided into three ranges (as a function of the statistical parameter *Rsk*) which depend on the examined edge geometry (Wiper geometry = -1…-0.2; Wiper & ISO geometry = -0.2…0.55; ISO geometry = 0.55…1). I showed that in fine turning a hitherto unknown range of the topological map (different from the ranges presented in the literature) can also be manufactured, and thus the expected characteristics of working surfaces can also be planned in the technological planning of fine turning. The investigated cutting parameter range and the conditions are identical to those in thesis 1.

Thesis III. is based on the following publications: [S2][S8][S15][S16]

Thesis 4.

I built a force model for the technology of fine turning in which I introduced l_{eff} – effective edge length, h_{eq} – equivalent chip thickness and $k_{1.0,1}$ – main specific cutting force. The dynamic model I introduced can estimate all three (F_c, F_f, F_p) cutting force components in the actual geometrical conditions of chip removal in technological planning. I designed, manufactured, and validated a special dynamometer for the range 0…100 N for fine turning technological experiments, and used it in my experiments.

Thesis IV. is based on the following publications: [S5][S10][S14]

8 Summary

In my dissertation I investigated the machinability of two widely used die-cast aluminium alloys (eutectic and hypereutectic) in the conditions of fine turning. I used diamond tools of three edge materials and two edge geometries.

I carried out the cutting experiments with design of experiments, after which I measured the surface roughness parameters *Ra* and *Rz* (which are widely used in industry). I performed the measurements twelve times on the surface of the workpiece 30 degrees intervals. I created a reduced (only containing significant effects) phenomenological model (with cutting parameters as input) for each tool and workpiece material to estimate surface roughness (altogether 20 equations). Then I created combined reduced phenomenological models which include workpiece materials and tool edge materials as qualitative variables.

I sought a cutting optimum (to minimize surface roughness in fine turning) with two methods, with target functions in the examined cutting parameter range with edge materials and workpiece materials used in the experiments. Then I performed measurements to validate the optimum.

I examined with grindings made from the cut surfaces (primary silicon near the cut surface) the cutting mechanism and roughness producing capacity of the tools of different edge geometries.

It is not enough to minimize surface roughness, its deviation also needs to be reduced therefore I also analysed the deviation of roughness parameters and came to the conclusion that it is the workpiece material that determines deviation.

Then I examined the statistical parameters of surface roughness (*Rsk*, *Rku*), which provide a preliminary characterization of the tribological behaviour of working surfaces. *Rsk*-*Rku* point pairs are called topological map in the literature. In the topological map distinct groups indicate different cutting technologies. My examinations showed that the roughness parameter *Rsk* depends on tool geometry. Based on edges, the topological map of fine turning that I examined can be divided into three distinct groups. In addition, with in addition, with a special edge geometry, a topological map not characteristic of turning different from the literature can also be “manufactured”. In other words, surfaces whose expected tribological behaviour during operation can be better (e.g. lower friction, less wear).

I also analysed the deviation of statistical parameters and similarly to *Ra* and *Rz*, I found that it is definitely determined by the workpiece materials.

After examining surface roughness, I analysed the dynamic conditions of the aluminium alloys during cutting. In fine turning, when the side cutting edge of the tool takes very little or no part in chip removal, (only the nose radius “works”) the dimensions of the resulting ship cross-section cannot be a defined in the conventional way (h – chip thickness, b – chip width). Therefore I introduced the parameters h_{eq} – equivalent chip thickness and l_{eff} - the cutting length of the edge of the tool, to geometrically characterize chip cross-sections in fine turning. Because of the usual sizes of chips in fine turning, I introduced a so-called $k_{1.0,1}$ parameter (main specific cutting force, where h_{eq} = 0.1 mm and l_{eff} = 1 mm). Then I created a new dynamic model with the new parameter.

I designed and adapted a special dynamometer for the examination of the dynamic conditions of fine turning. I modified a tool holder in such a way that the three component dynamometer cell was under the insert. Then I determined the sensitivity (pC/N) of the dynamometer in all three directions.

Of course, cutting is an eccentric load on the load cell. Therefore I performed a static check on the dynamometer system and took its error curves which have to be used to modify the measured values.

I worked out a measurement series and measured forces during cutting in the case of both workpiece materials. Dynamic measurements were performed twice, then their average was used for further evaluation. Based on the dynamic examinations, I determined the $k_{1.0,1}$ (main specific cutting force) values of both workpiece materials. Then I built a force model that fits all three cutting force components well.

9 Publications related to the dissertation

9.1 Journals

[S1] Horváth, R., Drégelyi-Kiss, Á.: Analysis of surface roughness of aluminum alloys fine turned: United phenomenological models and multi-performance optimization, *Measurement* 65 (2015) 181–192.
IF: 1.526.

[S2] Horváth, R., Czifra, Á., Drégelyi-Kiss, Á.: Effect of conventional and non-conventional tool geometries to skewness and kurtosis of surface roughness in case of fine turning of aluminium alloys with diamond tools, *The International Journal of Advanced Manufacturing Technology* (2014) 1-8
IF: 1.779.

[S3] Horváth, R., Mátyási, Gy., Drégelyi-Kiss, Á.: Optimization of machining parameters for fine turning operations based on the response surface method *ANZIAM Journal* 55 (2014) C250-C265.

[S4] Horváth, R., Drégelyi-Kiss, Á., Mátyási, Gy.: Application of RSM method for the examination of diamond tools, *Acta Polytechnica Hungarica* 11:(2) (2014) 137-147.
IF:0.471

[S5] Horváth, R.: A new model for fine turning forces, *Acta Polytechnica Hungarica* ***(accepted)***
IF:0.471.

[S6] Horváth, R., Mátyási, Gy., Drégelyi-Kiss, Á.: The examination of homogeneity in the fine turning of aluminium alloy, *Journal of Production Engineering* 17:(2) (2014) 35-39.

[S7] Horváth, R., Mátyási, Gy., Drégelyi-Kiss, Á.: Examination of the machinability of eutectic aluminium alloys, *Manufacturing Technology*

[S8] Horváth, R., Drégelyi-Kiss, Á., Mátyási, Gy.: The Examination of surface roughness parameters in the fine turning of hypereutectic aluminium alloys, *University POLITEHNICA of Bucharest Series D Mechanical Engineering*, ***(accepted)***

[S9] Horváth, R., Mátyási, Gy., Drégelyi-Kiss, Á.: The Examination of the Cutting Capacity of Different Aluminium Alloys with Statistical Methods, Using Different Edge Material Non-Conventional (Wiper) Edge Geometry Diamond Tools, *Materials Science Forum* 812 (2015) 71-76.

[S10] Horváth, R., Pálinkás, T., Mátyási, Gy.: Designing, making and adapting a dynamometer system to measure small forces forming during fine turning, *GÉP* 6 (2013) 48-53. (in Hungarian)
(Scientific Society for Mechanical Engineering - GTE, Technical Literature Prize 2013.)

9.2 Book chapter

[S11] Drégelyi-Kiss, Á., Horváth, R., Mikó, B.: Design of experiments (DOE) in investigation of cutting technologies In: Zebala W, Mankova I (szerk.) *Development in Machining Technology* Vol.3. Cracow: Cracow University of Technology Tadeusz Kosciuszko, (2013) 20-34.

9.3 Conference proceedings

[S12] Horváth, R., Drégelyi-Kiss, Á.: Analysis of surface roughness parameters in aluminium fine turning with diamond tool In: Ján Manka, Milan Tysler, Viktor Witkovsky, Ivan Frollo, *Measurement 2013 9th International Conference on Measurement.* Smolenice, Slovakia, 05.27.2013.-05.30.2013. Bratislava: Vydavatelstvo Slovenskej Akadémie Vied (VEDA), (2013) 275-278.

[S13] Horváth, R., Tóth-Laufer, E.: Fuzzy Model-Based Cutting Parameter Combination Optimization In: Szakál A *18th International Conference on Intelligent Engineering Systems - INES 2014.* (IEEE) Tihany, Hungary, 07.03.2014-07.05.2014. (2014) 151-155.

[S14] Horváth, R., Lukács, J.: Investigation of cutting forces on structural steel in case of fine turning, In: Bitay Enikő, *International Scientific Conference of Young Engineers XX.*, Cluj-Napoca, Romania, 03.19.2015.-03.20.2015. (2015) 167-170. (in Hungarian)

[S15] Horváth, R.: The examination of the statistical parameters of surface roughness during aluminium fine turning, In: Bitay Enikő, *International Scientific Conference of Young Engineers XIX.*, Cluj-Napoca, Romania, 03.20.2014.-03.21.2014. (2014) 205-207. (in Hungarian)

[S16] Horváth, R., Fazekas, A., Mátyási, Gy.: The examination of cutting ability of die-cast aluminium alloys, In: Bitay Enikő, *International Scientific Conference of Young Engineers XIX*. Cluj-Napoca, Romania, 03.20.2014-03.21.2014. (2014) 201-204. (in Hungarian)

[S17] Horváth, R., Mátyási, Gy.: The investigation of cuttingability of aluminium spare parts with help of design of experiments (DOE), In: Bitay Enikő, *International Scientific Conference of Young Engineers XVIII*. Cluj-Napoca, Romania, 03.21.2013.-03.22.2013. (2013) 159-163. (in Hungarian)